Title

Number and Brightness analysis of alpha-synuclein oligomerization and the associated mitochondrial morphology alterations in live cells

Journal

Biochimica et Biophysica Acta, 1840(6)

ISSN

0006-3002

Authors

Plotegher, N

Gratton, E

Bubacco, L

Publication Date

2014-06-01

DOI

10.1016/j.bbagen.2014.02.013

Peer reviewed

Published in final edited form as:
Biochim Biophys Acta. 2014 June ; 1840(6): 2014–2024. doi:10.1016/j.bbagen.2014.02.013.

Number and Brightness analysis of alpha-synuclein oligomerization and the associated mitochondrial morphology alterations in live cells

N. Plotegher[1], **E. Gratton**[2], and **L. Bubacco**[1,*]

[1]Department of Biology, University of Padova, Italy

[2]Laboratory for Fluorescence Dynamics, Department of Biomedical Engineering, University of California, Irvine, USA

Abstract

Background—Alpha-synuclein oligomerization is associated to Parkinson's disease etiopathogenesis. The study of alpha-synuclein oligomerization properties in live cell and the definition of their effects on cellular viability are among fields expected to provide the knowledge required to unravel the mechanism(s) of toxicity that lead to the disease.

Methods—We used Number and Brightness method, which is a method based on fluorescence fluctuation analysis, to monitor alpha-synuclein tagged with EGFP aggregation in living SH-SY5Y cells. The presence of alpha-synuclein oligomers detected with this method was associated with intracellular structure conditions, evaluated by fluorescence confocal imaging.

Results—Cells overexpressing alpha-synuclein-EGFP present a heterogeneous ensemble of oligomers constituted by less than 10 monomers, when the protein approaches a threshold concentration value of about 90 nM in the cell cytoplasm. We show that the oligomeric species are partially sequestered by lysosomes and that the mitochondria morphology is altered in cells presenting oligomers, suggesting that these mitochondria may be dysfunctional.

Conclusions—We showed that alpha-synuclein overexpression in SH-SY5Y causes the formation of alpha-synuclein oligomeric species, whose presence is associated with mitochondrial fragmentation and autophagic-lysosomal pathway activation in live cells.

General significance—The unique capability provided by the Number and Brightness analysis to study alpha-synuclein oligomers distribution and properties, and the study their association to intracellular components in single live cells is important to forward our understanding of the molecular mechanisms Parkinson's disease and it may be of general significance when applied to the study of other aggregating proteins in cellular models.

To whom correspondence should be addressed: Luigi Bubacco is to be contacted at the Department of Biology, University of Padua 35121 Padova (Italy). Phone number: +390498276346. luigi.bubacco@unipd.it.

Keywords

Fluorescence; oligomers; protein aggregation; lysosomes; Parkinson's disease; live imaging

1. Introduction

Parkinson's disease (PD) is the most common motor neurodegenerative disorder and it is associated to the prevalent death of the dopaminergic neurons in the *substantia nigra pars compacta* [1, 2].

A hallmark of PD is the presence of proteinaceous aggregates, termed Lewy bodies (LBs), in the surviving neurons in parkinsonians brains. The main constituent of LBs is a beta-sheet rich fibrillar form of alpha-synuclein (αsyn), a 140 amino acids protein mainly expressed at presynaptic terminals in mammalian brain, which is encoded by SNCA gene [3]. αSyn is a natively unfolded protein [4], but recently it was purified also in a purported alpha-helical homotetrameric conformation from cells and erythrocytes [5]. However, other laboratories failed to reproduce the results obtained by Bartels and co-workers [6], leaving the folding of the protein in the cellular environment under debate.

The presence of aggregated αsyn in LBs underlines the importance of this protein in the etiopathogenesis of PD. Moreover, single point mutations in SNCA gene (A30P, E46K, H50Q, G51D and A53T), gene duplication and triplication have been reported to cause autosomal dominant forms of PD [7–13].

The presence of fibrillar αsyn in parkinsonian's brains and the different propensity of the pathological mutants to aggregate observed *in vitro* [14, 15] imply that both the characterization of αsyn aggregation pathway(s) and the definition of αsyn oligomers and fibrils structures are crucial to unravel the mechanisms that link αsyn to cytotoxicity in PD.

However, the *in vitro* studies aimed to the characterization of the aggregation process, which were performed mainly by Circular Dichroism, fluorescence spectroscopy, NMR, atomic force microscopy and transmission electron microscopy [16], are strongly dependent on the experimental conditions used for the aggregation [17]. Consequentially, published results showed differences in both the kinetic properties of the process and the morphology of the aggregation products. Recently, a major effort has been put in the study of αsyn aggregation directly in cell models for PD, aiming to define the "in cells" aggregation, a choice that may also allow correlating a toxic effect to defined intermediate products of αsyn aggregation.

αSyn aggregation in cell models has been mostly studied using conventional microscopy techniques or transmission electron microscopy on fixed, antibody labeled and/or treated cells [18, 19]. Unfortunately, overexpression of αsyn by itself in most of the cellular models does not lead to the formation of detectable fibrils or inclusions. A good model to reproduce LBs like object in cells was recently produced by triggering the aggregation process with the addition of exogenous αsyn fibril fragments (seeds), which act as nucleation centers [18, 19] and induce the formation of large aggregates. This method, while probably relevant to the propagation of the disease, remains scarcely effective in the detection of the early stages of

αsyn oligomerization and in unraveling the toxic effects exerted by these αsyn aggregation products in live cells.

To take imaging analysis to a higher level of complexity, advanced fluorescence microscopy techniques have been applied to define the properties of the αsyn aggregation products. Bimolecular fluorescence complementation [20], fluorescence resonance energy transfer (FRET) [21], fluorescence recovery after photobleaching (FRAP), confocal fluorescence anisotropy measurements [22], allowed the visualization of αsyn oligomers in live cells, provided FRET efficiency, diffusion coefficients and fluorescence anisotropy of fluorophore-labeled αsyn aggregates or oligomers compared to αsyn monomers, respectively. These properties can provide information on the aggregates properties and on the protein localization. However, a more precise characterization of αsyn oligomerization is still required in order to correlate the diverse oligomeric species to their possible cellular toxicity.

In a recent paper [23], Ossato et al. used a new method, called Number and Brightness (N&B) fluctuation spectroscopy analysis, to study the aggregation process of exon1 of huntingtin. The N&B method is based on the analysis of the mean and the variance of fluorescence intensity distributions and allows measuring the number of molecules N and their brightness B at each pixel in a stack of images. The brightness B is directly related to the dimensions of the fluorescent molecules observed [24]. For this reason N&B method has been successfully used to study protein aggregation state in live cells [23, 25].

In this study we applied N&B analysis to obtain novel information on αsyn oligomerization in live cells. We evaluated αsyn oligomerization state, the oligomers subcellular localization and estimated the αsyn concentration required to initiate aggregation.

Having a quantitative method to study αsyn aggregation in live cells provides also an assay to associate αsyn oligomers to possible toxic effects. In particular, we focused on the effects due to the presence of αsyn oligomers on mitochondrial morphology, which has been previously related to αsyn overexpression in cell models [26, 27].

2. Materials and methods

2.1 Cell culture and transfections

SH-SY5Y neuroblastoma dopaminergic cell line was cultured in F12/DMEM media, with 10% FBS, 50 U/ml penicillin and 50 μg/ml streptomycin (GIBCO, Invitrogen), at 37°C in 5% CO_2. HEK293 cells were cultured in DMEM media, with 10% FBS, 50 U/ml penicillin and 50 μg/ml streptomycin (GIBCO, Invitrogen), at 37°C in 5% CO_2.

αSyn-EGFP plasmid was obtained by subcloning in a pEGFP-N1 vector (Clonetech) αsyn cDNA amplified by PCR with specific primers that introduced respectively at 5’ and at 3’ of the sequence, KpnI and BamHI recognition sites. A53T-EGFP plasmid was obtained by mutagenic PCR: to introduce the pathological single point mutation, properly designed primers (FOR 5’-gtggtgcatggtgtgacaacagtggctgag-3’ and REV 5’-

ctcagccactgttgtcacaccatgcaccac-3', Sigma Adrich) were used to amplify the αsyn-EGFP plasmid.

About $8.5 \cdot 10^5$ cells were plated in 35 mm dishes with a 14 mm microwell for imaging (MatTek, Ashland, MA, USA) and coated with fibronectin (Invitrogen); αsyn fused with EGFP (αsyn-EGFP) was then overexpressed using Lipofectamine (Invitrogen) as transfection reagent, following manufacturer protocol. The amount of plasmid was 1 μg (DNA:Lipofectamine = 1:5) in order to obtain in the expression an αsyn concentration that allows both αsyn aggregation and N&B analysis after imaging.

2.2 Lysosomes and mitochondria staining

Lysosome detection was performed using LysoTracker Red (Invitrogen) to a final concentration 100 nM in culture media for 45 minutes at 37° in 5% CO_2. Tetramethylrhodamine ethyl ester perchlorate (TMRE) (Sigma) was used to reveal mitochondria. Cells were incubated in a TMRE in culture media solution at a final concentration of 500 nM, for 30 minutes at 37° in 5% CO_2.

2.3 Cells treatments

To verify if N&B method is able to detect any variations in αsyn aggregation propensity due to exogenous treatments, cells were treated by dopamine, which is known to promote αsyn oligomerization, or by bafilomycin A 1, which is able to block autophagic lysosomal pathway. Dopamine was freshly prepared and transfected cells were treated for 3 hours with 100 μM dopamine. As reported by Klucken et al. (2012) [28], cells were treated overnight after transfection with 200 nM bafilomycin A 1.

2.4 Confocal microscopy

Confocal microscopy data were acquired with an Olympus FluoView1000 confocal laser scanning microscope, using an UPLSAPO 60 × water 1.2 NA objective.

N&B data were acquired using an excitation wavelength of 488 nm and laser power was set at 0.1%, corresponding to a laser power of 0.2 mW measured at the focal plane, and 100 frames were acquired for each cell, with a pixel dwell time of 20 μs. The image size was 256×256 pixels and the 100 images of each stack were acquired in about 2 minutes. Pixel size was set to be between 50 and 200 nm.

Signal from lysosomes or mitochondria, stained respectively with LysoTracker and TMRE, were collected using an excitation wavelength of 561 nm.

Filters were set to 505–525 nm for green channel or to 505–605 nm when two channels detection was needed and to 560–660 nm for the red channel.

At least 15 cells were imaged for each sample in 2 to 5 independent experiments. αsyn-EGFP oligomerization was measured in 5 different experiments, while staining with mitochondrial or lysosomal dyes were done in 3 experiments. A53T-EGFP overexpression, dopamine or Bafilomycin A 1 treatments were performed twice each.

2.5 Number and Brightness (N&B) analysis

N&B method is based on fluorescence fluctuation analysis and allows separating pixels with many dim molecules, from pixels with few bright molecules. The aggregation state of a protein is related to the first (average) and second moment (variance) of the fluorescence intensity distribution. Considering an average, a small variance corresponds to a large number of molecules that contribute to that average, while a large variance corresponds to few bright molecules. The mathematical equations that describe the relationship between the average ⟨k⟩ and the variance σ^2 of the intensity distribution and the apparent number of molecules N and the apparent brightness B for every pixel are:

$$N=\langle k\rangle^2/\sigma^2 \quad (1)$$

$$B=\sigma^2/\langle k\rangle \quad (2)$$

N and B values can be expressed in term of the number of particles (*n*) in the volume of excitation and the molecular brightness ε:

$$N=\varepsilon n/(\varepsilon+1) \quad (3)$$

$$B=\varepsilon+1 \quad (4)$$

The N and B values pixel per pixel and their distribution were obtained using SimFCS software (www.lfd.uci.edu). One of the parameter that has to be calibrated to use the method is the S_{factor}, which is related to the characteristics of the microscope. The S_{factor} obtained for the experiments described here with this instrumentation was 1.32 and is the parameter transforming the photocurrent in photon counts [23, 24].

The pixel dwell time is important in N&B analysis being the method based on fluctuation analysis. It should be shorter than the decay time of the fluctuations to obtain the variance associated to the brightness and the number of molecules in the focal volume (at 1 ms the fluctuations are elapsed), but longer than 1 μs to have fluctuations large enough to be informative [24].

The apparent brightness B of the molecules in cells is affected not only by the fluctuation due to fluorescence molecules movement, but also by photo bleaching and cell movements. To correct for these unwanted contributions a high pass filter algorithm (detrend filter) was applied to the stack of images. Detrend filter returns the average intensity at each pixel and deletes the fluctuations due to motion and photo bleaching that are slower than the particle fluctuation. The moving average parameter for the “detrend” filter, which is the number of frames used to calculate the average intensity to be added to each pixel intensity to filter out the unwanted contributions to fluorescence fluctuations should be maintained between 5 and 20 frames: we chose a moving average of 10, since in our experiments cell movements cause an intensity variation over a scale of about 10 frames.

For a detailed discussion on these parameters and their evaluation see Digman et al. (2008), Dalal et al. (2008) and Ossato et al. (2010) [23, 24, 29].

2.6 Calibration with monomeric EGFP

The laser power and the scanning conditions were calibrated transfecting SH-SY5Y with EGFP and measuring the brightness value B for the non-aggregating monomeric EGFP. The experiments to study the aggregation state of αsyn were then performed overexpressing αsyn-EGFP in the same cell line and using the same conditions.

The oligomers size *S* was then calculated considering the B value for the monomeric EGFP and the different brightness values for the oligomers:

$$S=(B_{oligomers}-1)/(B_{monomers}-1) \quad (5)$$

2.7 Calculating average concentration of αsyn in live cells

Considering the average N value we could estimate αsyn-EGFP concentration in each cell showing oligomeric species, which were 52% of the total observed cells in the 3 independent experiments. The calculation was performed using the mean N value for each cell obtained from the Gaussian fit of the N distribution calculated by SimFCS (Supplementary Figure S1); this N value is the mean apparent number of molecules in the focal volume of the microscope ($N_{average}$). To calculate the average molar concentration of αsyn molecules in a cell we use the following equation:

$$[\alpha syn]=N_{average}\cdot\gamma/N_{AVOGADRO}\cdot V_{focal} \quad (6)$$

The volume of the point spread function V_{focal} for a confocal microscope of about 0.2 femtoliter and a γ value of 0.353 were used to calculate the mean concentration of αsyn in the cells.

2.8 Mitochondria and lysosomes quantitative analysis

A tailored code (Matlab) for the quantitative analysis of mitochondria morphology and distribution in live cells was developed. After the selection of a threshold to eliminate the contribution due to the background of the TMRE stained mitochondria image, the distances among all pixels showing intensity above threshold were calculated to obtain a distribution representing the distance between pixels within mitochondria and among mitochondria, a parameter that could be associated to mitochondrial dimensions and distribution in the cell cytoplasm.

Oligomers, identified as pixels with B values higher than 1.34 (which is the average B value for monomers 1.18 plus its standard deviation 0.16) setting a threshold to this value for the analyzed B maps. After eliminating background contribution in the lysosomes images by setting an intensity threshold, we produced a new image in which pixel above the threshold in both images were colored in red, while the others in blue. The complete procedure is detailed in the Supplementary materials (Figure S3). The percentage of oligomers-positive

pixels that colocalize with lysosome over the total oligomers-positive pixels was calculated for the analyzed cells to quantify ALP activation.

3. Results

3.1 Instrument calibration and B value for monomeric EGFP

To evaluate the brightness (B) of monomeric EGFP, we overexpressed EGFP in SH-SY5Y cell line and acquire cell images under the conditions described in Materials and Methods section. The results allowed us to estimate the background contribution. After background correction, the B value solely due to monomeric EGFP in SH-SY5Y cells was estimated by averaging the B values obtained for EGFP in about 15 cells. Figure 1A shows the B distribution for EGFP in a representative cell. Fitting each cell histogram with a Gaussian distribution provided a mean value and a standard deviation for B:

$$B_{monomer} = 1.18 \pm 0.16$$

Figure 1B reports the B color map and the N color map for a representative analyzed cell. B map provides information on the distribution of B values in the cells: for EGFP transfected cells the B color map shows a homogeneous blue color, representing the average value obtained for the monomeric EGFP. The N map on the contrary is more heterogeneous, indicating a heterogeneous distribution of EGFP molecules in the cytoplasm. The intensity map and the N map are, as expected, similar, since the intensity per pixel in this situation is due to the monomeric EGFP molecules.

3.2 αSyn-EGFP overexpressing SH-SY5Y cells present monomeric and oligomeric αsyn

The time dependence of the fluorescence properties was investigated 24 hours after αsyn-EGFP transfection in SH-SY5Y: αsyn-EGFP aggregation was evaluated at 24 hours, 36 hours and 48 hours after transfection. Interestingly, at every time point cells in the same sample presented the same kind of heterogeneity in term of αsyn aggregates in cell cytoplasm.

A population of cells presented a B distribution centered at about 1.18, which is the B value characteristic of the monomeric EGFP and can be identified with monomeric αsyn-EGFP (Figure 2). From this result we hypothesized that the protein, at least in the conditions described here, is present as monomer in the cytoplasm. 24 hours after the transfection it was possible to identify in some cells by N&B analysis, pixels presenting not only a B value characteristic of the monomer, but also higher B values, compatible with oligomeric species.

Using $B_{monomer}$ value as reference, we were able to identify cells presenting oligomeric species from the brightness values. As can be seen in Figure 3A, the distribution of the brightness for the representative cell transfected with αsyn-EGFP starts to broaden and in Figure 3B a more pronounced broadening is observed. When a pixel shows B values higher than $B_{monomer}$ it indicates that at least some of the fluorescence in that pixel can be assigned to αsyn-EGFP oligomers. A gallery of images representing different cells and the related B

maps presenting B values corresponding to oligomeric αsyn-EGFP are shown in the Supplementary Figure S4.

The distribution of brightness values for part of the imaged cells were very different and not well separated from the Gaussian distribution centered on 1.18 representing the monomeric αsyn-EGFP. Moreover, it was not possible to separate the contribution of oligomers with different dimensions; accordingly, the standard deviation of the B values for the oligomeric species is 4-fold larger than the standard deviation of the B distribution of monomeric αsyn-EGFP. With this premise, we can only obtain an estimate of the mean brightness of the entire heterogeneous ensemble. Considering different cells and different experiments, we calculated a weighted average of the brightness of the entire ensemble of oligomeric species, as described in the Materials and Methods section, that is:

$$B = 1.98 \pm 0.65$$

The equation 5, describing the relationship between the B values measured with N&B for a monomer and for oligomeric species and the aggregation size, allowed us to calculate the mean dimension of the oligomers found in αsyn-EGFP transfected SH-SY5Y cells. On average, the oligomeric species are constituted by 6±4 αsyn monomers, which is in good agreement with a very recent estimate on αsyn early oligomers produced *in vitro* and observed with single molecules fluorescence techniques (n≤10) [30].

Imaging the cells at different time points after the transfection did not influence the percentage of pixels showing oligomeric species that were detected: from about 8% to 30% in different cells. This result suggests that both the B value, i.e. the average dimension of αsyn oligomers and the average percentage of pixels in cells presenting oligomers are probably dependent on the protein concentration or on the activation of cellular clearance mechanism(s) that can target both αsyn monomers or oligomers leading to a reduction of their amount in the cell cytoplasm.

As a control, the experiments mentioned above were also performed in HEK293 cells obtaining comparable results both in term of αsyn-EGFP oligomers dimension and distribution. Therefore, we concluded that as detected by the N&B method, the conditions that may differ between the two tested cell lines are not determinant in the aggregation process and proceeded by testing only the neuroblastoma cell line SH-SY5Y.

3.3 Estimation of the αsyn concentration threshold for oligomerization

We estimated the mean αsyn concentration in cell cytoplasm for different cells overexpressing αsyn-EGFP as described in the Materials and Methods section. Surprisingly, while the percentage of pixels showing oligomeric species in all analyzed cell is significantly variable, the mean concentration of αsyn calculated from the average N value in these cells showing oligomers is around 175 nM (about 178±39 nM). Moreover, looking at all the cells, we found a reasonable value for the threshold concentration needed for the protein to form oligomers, which is about 90 nM. In the cells where a large part of pixels showed the presence of αsyn oligomers or a very high αsyn concentration, we could not observe a conversion of the oligomeric species into fibrillar structure or larger inclusions,

consistently with what is reported in the literature concerning αsyn aggregation in cell models [20, 21, 31].

3.4 Oligomers are localized in specific regions of the cell

Looking at the B map for the cells presenting oligomers (Figure 3D), it is clear that the distribution of pixels showing brighter particles is not homogeneous. The clustering of the pixels presenting oligomeric species in specific regions of the cell cytoplasm could suggest that there is a scaffolding effect: the oligomers could be bound to intracellular structures, i.e. organelles, or be sequestered by lysosomes. Part of the oligomers seems also to be localized at the inner side of the plasma membrane.

The movements of the cell membranes or organelles where αsyn molecules can be bound may affect the calculation of the brightness, causing an increase in the variance of the fluorescence intensity distribution. To verify that the increase of the B values is due to the formation of αsyn oligomeric species and not to motion artifacts, a “detrend” filter was applied to the images to obtain the B distribution and B map. This filter computationally removes the contributions due to the photo bleaching and to slow-movements associated to larger structures movements inside the cell [23]. The increase in the B value due to the fraction of αsyn-EGFP that is bound to membranes [32, 33] because of the membranes movements was removed by the “detrend” filter. To further verify the complete removal of unwanted contribution to B value calculation due to slow movements, an algorithm that calculates the derivative of each stack of images and shows, pixel per pixel, the movements of the cell and inside the cell was used (Figure S5).

Interestingly, the N&B analysis showed that the regions where brightness B is higher, the value of N decreases (Figure 2D), suggesting that in those pixels there are more oligomeric species, but fewer particles. This lower value for N observed in correspondence of high B values could account for a scaffolding effect, due to the sequestration of the oligomers into lysosomes [34] or exosomes [35], or to their binding to mitochondria [26, 36].

Another possible explanation of low N value in these regions is that the αsyn oligomers could incorporate other proteins that are invisible to N&B technique being non-fluorescent; therefore, these oligomers containing αsyn and also other proteins can occupy more space in the cell cytoplasm leading to the features we detect calculating N and B maps. The capability of amyloid forming protein to sequester cytoplasmic proteins when aggregating was reported for chimeric β-sheet amyloidogenic proteins [37] and is supported by the presence of soluble complexes containing αsyn and 14-3-3 proteins in cultured human dopaminergic neurons [38] and in a A53T transgenic mice model [39].

3.5 αSyn-EGFP oligomers are partially sequestered by lysosomes

To verify if the confinement effect observed for the αsyn’s signal while comparing the B and the N maps of the cells presenting oligomers could be due to the presence of lysosomes sequestration, we stained EGFP and αsyn-EGFP overexpressing cells with LysoTracker Red. From the B map for αsyn-EGFP cells and the LysoTracker-stained lysosomes image (Figure 4C and 4D) it is clear that there is a partial overlap. Colocalization analysis, as represented in Supplementary figure S3, showed that about 25% of the pixels presenting B

values corresponding to αsyn oligomeric species (higher than 1.34) colocalize with lysosomes. This result suggests that αsyn oligomers are partially sequestered into lysosomes and lead to the activation of the autophagic-lysosomal pathway (ALP) that is believed to be responsible for the clearance of misfolded αsyn [34, 40]. Noteworthy is the fact that in lysosomes pH is around 5.0. This pH value can induce the quenching of EGFP fluorescence [41] and influence the N and B values estimation. However, the control performed on cells transfected with monomeric EGFP and stained with LysoTracker (Figure S6) does not show any consistent variation in the brightness of the monomeric EGFP colocalized with lysosomes. Therefore, the pH quenching effect may induce (if any) only a mild underestimate of the B values, which cannot account for the higher brightness values due to αsyn oligomeric species.

To further test if lysosomes movements could affect the B value detected in αsyn overexpressing cells, we evaluated the efficacy of the “detrend” filter by comparing the B maps obtained with or without detrending (Figure S7). These results suggest that the filter is able to remove the contribution due to cells and organelles movements, leading to a proper evaluation of B values for monomeric EGFP and oligomeric αsyn-EGFP.

3.6 Alterations in mitochondria characteristics are due to αsyn oligomers

As can be seen in Figure 4, not all the pixels presenting oligomeric species are enclosed into lysosomes, accounting for a possibly progressive activation of the clearance system. In 2010 Nakamura and co-workers [26] proposed that one possible damaging mechanism that could be ascribed to αsyn is its direct interaction with mitochondrial membranes. They showed that αsyn overexpression causes mitochondrial fragmentation, but they could not verify the conformation that αsyn acquired while damaging mitochondria. Furthermore, they previously showed by FRET that there is a specific interaction between αsyn and mitochondrial membranes [36], as reported also using an *in vitro* approach [42].

On these premises, the possibility of a damaging effect due to αsyn oligomers on mitochondrial characteristics was explored. To this aim, mitochondria were stained with a mitochondrial dye (TMRE) to verify whether the presence of oligomers could be related to the mitochondrial fragmentation as previously suggested by Nakamura et al. [26]. Figure 5 shows an example of a cell overexpressing EGFP or αsyn-EGFP, where pixels presenting oligomeric species were identified. The comparison between mitochondria stained with TMRE in cells overexpressing EGFP or showing αsyn-EGFP oligomers is shown in Figure 5C. The difference in mitochondrial morphology and distribution is clear, but a more precise quantification of these variations is presented in Figure 6. The distribution of distances between pixels that constitute mitochondria were calculated as described in the Materials and Methods paragraph and reported in the graph for the two different cases. The histograms carry the information about the distribution of the mitochondria in the cell and about their dimensions. As shown, when αsyn oligomers are present, the organelles are smaller and less spread in the cell cytoplasm, suggesting that they underwent fragmentation, in agreement with previous publications [26, 43, 44]. On the contrary, this result is apparently in contrast with another study reporting the absence of mitochondrial morphology alterations in SH-SY5Y cells overexpressing αsyn [45].

TMRE allows not only identifying mitochondria, but also to measure their membrane potentials through Nernst equation. As published by Nakamura et al. [26], we could not detect any difference in the mitochondrial potential based on this experiment.

3.7 Agents that may promote αsyn-EGFP oligomerization in live cells

The possibility of using N&B to evaluate differences in the aggregation products found in live cells was explored. We first treat asyn-EGFP overexpressing cells and EGFP overexpressing cells as control with dopamine, which is known to lead to the formation of stable αsyn oligomeric species [46]. As reported in Figure S8, SH-SY5Y overexpressing cells treated with dopamine did not show a considerable difference in term of oligomers dimensions. Another possibility we explored was to overexpress A53T-EGFP pathological mutant, which is known to have an increased aggregation propensity compared to wild-type αsyn [14]. Also in this case, the B values obtained are similar with the ones obtained in αsyn-EGFP overexpressing cells (Figure S9), suggesting that at the earliest stages of the aggregation process the mutations does not affect the oligomers properties in live cells.

To further understand which are the mechanisms associated with αsyn aggregation, we inhibited autophagy using bafilomycin A 1 and verify if any variation in oligomers size or amount could be measured. As previously published [28], we observed a consistent cell death, while surviving cells showed αsyn-EGFP concentration lower than 90 nM, which is the limit to observe the oligomeric species we previously identified in untreated samples.

4. Discussion

αSyn aggregation process is widely studied *in vitro*, but the results obtained are strongly dependent on the experimental conditions. Moreover, the transient oligomers and aggregates *in vitro* cannot be isolated to relate these to possible mechanism(s) of toxicity. Recently, some studies have been performed in cellular models, providing more relevant but still not conclusive results. In particular, a more precise characterization of αsyn aggregates dimensions and aggregates related toxicity is still lacking. In this context, N&B method emerges as a powerful tool to study αsyn aggregation state in live cell. The physiological state of the protein was characterized in the dopaminergic neuroblastoma SH-SY5Y cell line overexpressing αsyn-EGFP. It was observed that αsyn is mainly present as a monomer in cell cytoplasm, at least under the experimental conditions tested here. It may be questioned that the presence of EGFP at the C-terminus of αsyn interferes with a possible folding into the tetramer reported in the literature [5]. However, it has been shown that the region involved in the interactions that lead to the αsyn tetramer is the folded N-terminus [47], while the C-terminus where the EGFP is fused in our system is unfolded and free to move also in the proposed tetrameric conformation, suggesting that the tag is not likely to hinder the purported quaternary structure of the protein. Therefore, we concluded that in our cellular model αsyn is monomeric when its concentration is below 90 nM, while it starts oligomerizing at higher cytoplasmic concentration.

The measured threshold concentration seems to be quite low compared to the values reported for αsyn concentration in neurons, which is in the micromolar range [30, 48]. However, αsyn concentration in neurons is mainly estimated as 0.5%–1% of total soluble

brain proteins as evaluated by western blot of brain homogenate [49, 50] and, to the best of our knowledge, no direct measurements of αsyn concentration in neurons are available.

It should also be mentioned that a plausible interpretation of the differences between the N&B measured concentration and the estimated physiological αsyn concentration in neurons is the partition of the protein between cellular cytosol and neuronal membranes. It is known that alphasynuclein can efficiently bind to lipid membranes [32] and to SNARE-protein vesicle-associated membrane protein 2 [51] to promote SNARE-complex assembly in neurons. It follows that total αsyn concentration in neurons may result higher than the value we reported for our cellular model in which the method used (N&B, based on fluctuations) only detects the molecules that are mobile in the cell justifying the discrepancy between the two reported concentrations. The average αsyn concentration in cells showing oligomeric species is around 175 nM, which is a concentration below the upper limit of the N&B method sensitivity (about 1 μM). The detected oligomers are present 24 hours after the transfection and their presence can be associated to mitochondrial fragmentation. However, we cannot determine unambiguously if the oligomers directly damage mitochondrial membranes or if other mechanisms are involved.

Based on these data, we propose that the concentration of αsyn-EGFP in cell cytoplasm and the formation of nucleation centers that trigger the aggregation are the two key factors in the aggregation in cell cytoplasm. These results are in good agreement with the findings that the level of αsyn in neurons is crucial for the onset of PD, because duplication and triplication of *SNCA* gene, encoding for αsyn lead to severe and early onset PD forms [10, 13].N&B method allowed us to characterize the average dimension of αsyn oligomers, which are constituted by 6±4 αsyn monomers. However, the distributions of B values reflecting αsyn oligomers dimensions are very broad, meaning that the ensemble of oligomeric species is heterogeneous. The heterogeneity is also a characteristic of the oligomeric species obtained *in vitro*, but in those experiments it may be difficult to discriminate between the intrinsic heterogeneity of the sample and the one induced by the experimental conditions [17]. In a very recent paper [30], the very early αsyn oligomers obtained *in vitro* were studied using a direct single molecule fluorescence technique. Cremades and co-workers could estimate with a direct method the number of αsyn monomers that constitute these first oligomers, i.e. less than 10 molecules. However, in the literature the number of monomers in oligomeric species obtained under different experimental conditions *in vitro* and detected with different indirect techniques (as gel filtration or small angle X-ray scattering) can vary up to about 100 αsyn monomers [30, 52–54]. For this reason, we believe that the most relevant results are obtained in live cells without isolating oligomers, which *per se* may induce αsyn oligomeric species modifications.

It is worth noting that αsyn oligomers could incorporate other proteins present in the cell cytoplasm that co-aggregate with αsyn [38, 39], producing larger aggregates. These molecules go undetected because they are invisible to the technique presented here. Moreover, the N&B method measures the average brightness of the particles in the volume of excitation. If the distribution is very skewed toward few large oligomers, the method will tend to underestimate the contribution of these large particles.

Interestingly, we could not find any larger aggregates or fibrils in the cells we examined. This result is in agreement with previous experiments reported in the literature [20, 21, 31] and suggests that αsyn oligomers, being the most toxic species [55], may induce cell death [56] earlier than forming larger aggregates, at least in this PD cell model. A possibility is that the rate of the oligomers formation in this model is much faster, because of αsyn-EGFP overexpression, than the rate in neurons in parkinsonian brains. A large amount of oligomers in these SH-SY5Y overexpressing αsyn leads to cell death, overwhelming the defense mechanisms before αsyn fibrils and LBs can be formed.

A higher aggregation rate and an associated higher toxicity in live cells may also be present in Bafilomycin A 1 and dopamine treated cells, partially explaining the absence of any difference between the treated or untreated samples. The same can be observed for A53T-EGFP overexpressing cells, suggesting that the characterization of oligomers differences at the early steps of the aggregation process in these different conditions is not trivial, especially in live cells. As shown in the B map in Figure 3D, αsyn oligomers localize in certain cell regions. Considering the ability of αsyn to bind to membranes characterized by different lipid compositions [57], a “scaffolding effect” may be envisioned, partially due to the localization of αsyn oligomers at the numerous membranous structures present in the cell cytoplasm and at the plasma membrane. This interpretation is supported by a model for αsyn aggregation where the early αsyn oligomers are formed not only in the cell cytoplasm but also at the membranes [32, 58], which can lead to calcium leakage [59] and to synaptic vesicles homeostasis disruption in neurons [60].

Another explanation for this pattern is the sequestration of the toxic oligomeric species by lysosomes. In the recent literature, several evidences support involvement of ALP in αsyn clearance [34, 40]. After staining αsyn-EGFP overexpressing SH-SY5Y cells with Lysotracker, we find that part of the oligomers present in cells cytoplasm co-localize with lysosomes, as shown in a mice model by Mak et al. (2010) [34], supporting the activation of ALP when these first toxic species form.

It is known that the acidic pH can quench EGFP fluorescence [41] and that pH is about 4.8 in the lysosomes. The effect on N&B estimations due to EGFP quenching at acidic pH is that the brightness of the EGFP is lowered, leading to an underestimation of the actual B value for αsyn oligomers in the lysosomes. However, not all the oligomeric species that we identified by N&B method were cleared by ALP and we tried to identify possible toxic effects due to their presence in cell cytoplasm. Looking for elective targets for oligomeric species, we stained αsyn-EGFP overexpressing cells with a mitochondrial dye and compared their mitochondria morphology with cells overexpressing EGFP. In the recent past several studies associated αsyn toxicity to mitochondria: Nakamura and co-workers showed how αsyn overexpression leads to mitochondria fragmentation by a direct interaction using fluorescence imaging techniques and highly resolved transmission electron microscopy. They hypothesized that the variations in mitochondria morphology are due to the direct interaction of αsyn oligomers with mitochondrial membranes. This idea is further supported by the evidence of αsyn interaction with mitochondria [36] and localization of αsyn at membranes mimicking mitochondrial membranes [42] or within mitochondria [61]. Moreover, it was proposed that αsyn can inhibit mitochondrial fusion processes, again

because of the protein special interactions with mitochondrial membranes [43] or that mitochondrial fission is increased through an increased Drp1 translocation to mitochondria due to αsyn overexpression [62].

The mitochondrial fragmentation due to αsyn is associated with respiration impairments after 48 hours from the transfection [26], but also with limitations in mitochondria dynamics in the cell [44]. Moreover, asyn can translocate to mitochondria and accumulate, causing complex I impairment [61, 63].

Our results, showing mitochondrial fragmentation, are in agreement with the literature [26, 43, 44, 62, 64], excluding Zhu et al. (2012) [45]. Moreover, our data suggest that there is a relationship between the presence of αsyn oligomers in the cytoplasm and variations in mitochondria morphology, while others could only establish a link between αsyn overexpression and mitochondria conditions. Therefore, based on the result presented in the literature and on the data reported in this manuscript, it is rather established that αsyn induces mitochondrial fragmentation, but still unclear is the precise mechanism(s) by which this damaging occurs. Direct αsyn-mitochondria interactions, alterations in mitochondrial fusion-fission mechanisms due to αsyn overexpression or aggregation and other indirect mechanisms that alter mitochondrial morphology cannot be mutually excluded.

5. Conclusion

Our results indicate that αsyn can oligomerize when it is overexpressed in SH-SY5Y cell line and αsyn concentration in cell cytoplasm is at least 90 nM. We show that αsyn oligomers constituted by 6±4 monomers may be partially sequestered into lysosomes and their presence in live cells is associated with mitochondrial morphology alterations, suggesting a putative role for these oligomeric species in mitochondrial dysfunction in PD.

Supplementary Material

Refer to Web version on PubMed Central for supplementary material.

Acknowledgments

Thanks are due to M. Stakic and C. Chiu for assistance with the experiments and to E. Greggio for the valuable discussions. We also acknowledge “Fondazione Ing. Aldo Gini” for funding N. Plotegher experience at the Laboratory for Fluorescence Dynamics (University of California, Irvine). This work is supported in part by NIH-P41 P41-RRO3155, NIH-P41 GM103540 and NIH P50-GM076516 (EG).

Abbreviations

N&B	Number and Brightness
PD	Parkinson’s disease
αsyn	alpha-synuclein
LBs	Lewy bodies
TMRE	tetramethylrhodamine ethyl ester perchlorate

ALP autophagic-lysosomal pathway.

References

1. Samii A, Nutt JG, Ransom BR. Parkinson's disease. Lancet. 2004; 363:1783–1793. [PubMed: 15172778]
2. de Lau LM, Breteler MM. Epidemiology of Parkinson's disease. Lancet Neurol. 2006; 5:525–535. [PubMed: 16713924]
3. Spillantini MG, Crowther RA, Jakes R, Hasegawa M, Goedert M. alpha-Synuclein in filamentous inclusions of Lewy bodies from Parkinson's disease and dementia with lewy bodies. Proc Natl Acad Sci U S A. 1998; 95:6469–6473. [PubMed: 9600990]
4. Weinreb PH, Zhen W, Poon AW, Conway KA, Lansbury PT Jr. NACP, a protein implicated in Alzheimer's disease and learning, is natively unfolded. Biochemistry. 1996; 35:13709–13715. [PubMed: 8901511]
5. Bartels T, Choi JG, Selkoe DJ. alpha-Synuclein occurs physiologically as a helically folded tetramer that resists aggregation. Nature. 2011; 477:107–110. [PubMed: 21841800]
6. Fauvet B, Mbefo MK, Fares MB, Desobry C, Michael S, Ardah MT, Tsika E, Coune P, Prudent M, Lion N, Eliezer D, Moore DJ, Schneider B, Aebischer P, El-Agnaf OM, Masliah E, Lashuel HA. alpha-Synuclein in central nervous system and from erythrocytes, mammalian cells, and Escherichia coli exists predominantly as disordered monomer. J Biol Chem. 2012; 287:15345–15364. [PubMed: 22315227]
7. Polymeropoulos MH, Lavedan C, Leroy E, Ide SE, Dehejia A, Dutra A, Pike B, Root H, Rubenstein J, Boyer R, Stenroos ES, Chandrasekharappa S, Athanassiadou A, Papapetropoulos T, Johnson WG, Lazzarini AM, Duvoisin RC, Di Iorio G, Golbe LI, Nussbaum RL. Mutation in the alphasynuclein gene identified in families with Parkinson's disease. Science. 1997; 276:2045–2047. [PubMed: 9197268]
8. Kruger R, Kuhn W, Muller T, Woitalla D, Graeber M, Kosel S, Przuntek H, Epplen JT, Schols L, Riess O. Ala30Pro mutation in the gene encoding alpha-synuclein in Parkinson's disease. Nat Genet. 1998; 18:106–108. [PubMed: 9462735]
9. Zarranz JJ, Alegre J, Gomez-Esteban JC, Lezcano E, Ros R, Ampuero I, Vidal L, Hoenicka J, Rodriguez O, Atares B, Llorens V, Gomez Tortosa E, del Ser T, Munoz DG, de Yebenes JG. The new mutation, E46K, of alpha-synuclein causes Parkinson and Lewy body dementia. Ann Neurol. 2004; 55:164–173. [PubMed: 14755719]
10. Chartier-Harlin MC, Kachergus J, Roumier C, Mouroux V, Douay X, Lincoln S, Levecque C, Larvor L, Andrieux J, Hulihan M, Waucquier N, Defebvre L, Amouyel P, Farrer M, Destee A. Alpha-synuclein locus duplication as a cause of familial Parkinson's disease. Lancet. 2004; 364:1167–1169. [PubMed: 15451224]
11. Kiely AP, Asi YT, Kara E, Limousin P, Ling H, Lewis P, Proukakis C, Quinn N, Lees AJ, Hardy J, Revesz T, Houlden H, Holton JL. alpha-Synucleinopathy associated with G51D SNCA mutation: a link between Parkinson's disease and multiple system atrophy? Acta Neuropathol. 2013; 125:753–769. [PubMed: 23404372]
12. Proukakis C, Dudzik CG, Brier T, MacKay DS, Cooper JM, Millhauser GL, Houlden H, Schapira AH. A novel alpha-synuclein missense mutation in Parkinson disease. Neurology. 2013; 80:1062–1064. [PubMed: 23427326]
13. Singleton AB, Farrer M, Johnson J, Singleton A, Hague S, Kachergus J, Hulihan M, Peuralinna T, Dutra A, Nussbaum R, Lincoln S, Crawley A, Hanson M, Maraganore D, Adler C, Cookson MR, Muenter M, Baptista M, Miller D, Blancato J, Hardy J, Gwinn-Hardy K. alpha-Synuclein locus triplication causes Parkinson's disease. Science. 2003; 302:841. [PubMed: 14593171]
14. Li J, Uversky VN, Fink AL. Effect of familial Parkinson's disease point mutations A30P and A53T on the structural properties, aggregation, and fibrillation of human alpha-synuclein. Biochemistry. 2001; 40:11604–11613. [PubMed: 11560511]

15. Fredenburg RA, Rospigliosi C, Meray RK, Kessler JC, Lashuel HA, Eliezer D, Lansbury PT Jr. The impact of the E46K mutation on the properties of alpha-synuclein in its monomeric and oligomeric states. Biochemistry. 2007; 46:7107–7118. [PubMed: 17530780]
16. Bisaglia M, Mammi S, Bubacco L. Structural insights on physiological functions and pathological effects of alpha-synuclein. FASEB J. 2009; 23:329–340. [PubMed: 18948383]
17. Giehm L, Lorenzen N, Otzen DE. Assays for alpha-synuclein aggregation. Methods. 2011; 53:295–305. [PubMed: 21163351]
18. Luk KC, Song C, O'Brien P, Stieber A, Branch JR, Brunden KR, Trojanowski JQ, Lee VM. Exogenous alpha-synuclein fibrils seed the formation of Lewy body-like intracellular inclusions in cultured cells. Proc Natl Acad Sci U S A. 2009; 106:20051–20056. [PubMed: 19892735]
19. Nonaka T, Watanabe ST, Iwatsubo T, Hasegawa M. Seeded aggregation and toxicity of {alpha}-synuclein and tau: cellular models of neurodegenerative diseases. J Biol Chem. 2010; 285:34885–34898. [PubMed: 20805224]
20. Outeiro TF, Putcha P, Tetzlaff JE, Spoelgen R, Koker M, Carvalho F, Hyman BT, McLean PJ. Formation of toxic oligomeric alpha-synuclein species in living cells. PLoS One. 2008; 3:e1867. [PubMed: 18382657]
21. Roberti MJ, Bertoncini CW, Klement R, Jares-Erijman EA, Jovin TM. Fluorescence imaging of amyloid formation in living cells by a functional, tetracysteine-tagged alpha-synuclein. Nat Methods. 2007; 4:345–351. [PubMed: 17351621]
22. Roberti MJ, Jovin TM, Jares-Erijman E. Confocal fluorescence anisotropy and FRAP imaging of alpha-synuclein amyloid aggregates in living cells. PLoS One. 2011; 6:e23338. [PubMed: 21858077]
23. Ossato G, Digman MA, Aiken C, Lukacsovich T, Marsh JL, Gratton E. A two-step path to inclusion formation of huntingtin peptides revealed by number and brightness analysis. Biophys J. 2010; 98:3078–3085. [PubMed: 20550921]
24. Digman MA, Dalal R, Horwitz AF, Gratton E. Mapping the number of molecules and brightness in the laser scanning microscope. Biophys J. 2008; 94:2320–2332. [PubMed: 18096627]
25. Vetri V, Ossato G, Militello V, Digman MA, Leone M, Gratton E. Fluctuation methods to study protein aggregation in live cells: concanavalin A oligomers formation. Biophys J. 2011; 100:774–783. [PubMed: 21281593]
26. Nakamura K, Nemani VM, Azarbal F, Skibinski G, Levy JM, Egami K, Munishkina L, Zhang J, Gardner B, Wakabayashi J, Sesaki H, Cheng Y, Finkbeiner S, Nussbaum RL, Masliah E, Edwards RH. Direct membrane association drives mitochondrial fission by the Parkinson disease-associated protein alpha-synuclein. J Biol Chem. 2011; 286:20710–20726. [PubMed: 21489994]
27. Chinta SJ, Mallajosyula JK, Rane A, Andersen JK. Mitochondrial alpha-synuclein accumulation impairs complex I function in dopaminergic neurons and results in increased mitophagy in vivo. Neurosci Lett. 2010; 486:235–239. [PubMed: 20887775]
28. Klucken J, Poehler AM, Ebrahimi-Fakhari D, Schneider J, Nuber S, Rockenstein E, Schlotzer-Schrehardt U, Hyman BT, McLean PJ, Masliah E, Winkler J. Alpha-synuclein aggregation involves a bafilomycin A 1-sensitive autophagy pathway. Autophagy. 2012; 8:754–766. [PubMed: 22647715]
29. Dalal RB, Digman MA, Horwitz AF, Vetri V, Gratton E. Determination of particle number and brightness using a laser scanning confocal microscope operating in the analog mode. Microsc Res Tech. 2008; 71:69–81. [PubMed: 17937391]
30. Cremades N, Cohen SI, Deas E, Abramov AY, Chen AY, Orte A, Sandal M, Clarke RW, Dunne P, Aprile FA, Bertoncini CW, Wood NW, Knowles TP, Dobson CM, Klenerman D. Direct observation of the interconversion of normal and toxic forms of alpha-synuclein. Cell. 2012; 149:1048–1059. [PubMed: 22632969]
31. Klucken J, Outeiro TF, Nguyen P, McLean PJ, Hyman BT. Detection of novel intracellular alpha-synuclein oligomeric species by fluorescence lifetime imaging. FASEB J. 2006; 20:2050–2057. [PubMed: 17012257]
32. Auluck PK, Caraveo G, Lindquist S. alpha-Synuclein: membrane interactions and toxicity in Parkinson's disease. Annu Rev Cell Dev Biol. 2010; 26:211–233. [PubMed: 20500090]

33. Yang ML, Hasadsri L, Woods WS, George JM. Dynamic transport and localization of alpha-synuclein in primary hippocampal neurons. Mol Neurodegener. 2010; 5:9. [PubMed: 20181133]
34. Mak SK, McCormack AL, Manning-Bog AB, Cuervo AM, Di Monte DA. Lysosomal degradation of alpha-synuclein in vivo. J Biol Chem. 2010; 285:13621–13629. [PubMed: 20200163]
35. Emmanouilidou E, Melachroinou K, Roumeliotis T, Garbis SD, Ntzouni M, Margaritis LH, Stefanis L, Vekrellis K. Cell-produced alpha-synuclein is secreted in a calcium-dependent manner by exosomes and impacts neuronal survival. J Neurosci. 2010; 30:6838–6851. [PubMed: 20484626]
36. Nakamura K, Nemani VM, Wallender EK, Kaehlcke K, Ott M, Edwards RH. Optical reporters for the conformation of alpha-synuclein reveal a specific interaction with mitochondria. J Neurosci. 2008; 28:12305–12317. [PubMed: 19020024]
37. Olzscha H, Schermann SM, Woerner AC, Pinkert S, Hecht MH, Tartaglia GG, Vendruscolo M, Hayer-Hartl M, Hartl FU, Vabulas RM. Amyloid-like aggregates sequester numerous metastable proteins with essential cellular functions. Cell. 2011; 144:67–78. [PubMed: 21215370]
38. Xu J, Kao SY, Lee FJ, Song W, Jin LW, Yankner BA. Dopamine-dependent neurotoxicity of alpha-synuclein: a mechanism for selective neurodegeneration in Parkinson disease. Nat Med. 2002; 8:600–606. [PubMed: 12042811]
39. Shirakashi Y, Kawamoto Y, Tomimoto H, Takahashi R, Ihara M. alpha-Synuclein is colocalized with 14-3-3 and synphilin-1 in A53T transgenic mice. Acta Neuropathol. 2006; 112:681–689. [PubMed: 16957925]
40. Ebrahimi-Fakhari D, Wahlster L, McLean PJ. Protein degradation pathways in Parkinson's disease: curse or blessing. Acta Neuropathol. 2012; 124:153–172. [PubMed: 22744791]
41. Patterson GH, Knobel SM, Sharif WD, Kain SR, Piston DW. Use of the green fluorescent protein and its mutants in quantitative fluorescence microscopy. Biophys J. 1997; 73:2782–2790. [PubMed: 9370472]
42. Zigoneanu IG, Yang YJ, Krois AS, Haque E, Pielak GJ. Interaction of alpha-synuclein with vesicles that mimic mitochondrial membranes. Biochim Biophys Acta. 2012; 1818:512–519. [PubMed: 22155643]
43. Kamp F, Exner N, Lutz AK, Wender N, Hegermann J, Brunner B, Nuscher B, Bartels T, Giese A, Beyer K, Eimer S, Winklhofer KF, Haass C. Inhibition of mitochondrial fusion by alpha-synuclein is rescued by PINK1, Parkin and DJ-1. EMBO J. 2010; 29:3571–3589. [PubMed: 20842103]
44. Xie W, Chung KK. Alpha-synuclein impairs normal dynamics of mitochondria in cell and animal models of Parkinson's disease. J Neurochem. 2012; 122:404–414. [PubMed: 22537068]
45. Zhu M, Li W, Lu C. Role of alpha-synuclein protein levels in mitochondrial morphology and cell survival in cell lines. PLoS One. 2012; 7:e36377. [PubMed: 22558453]
46. Yamakawa K, Izumi Y, Takeuchi H, Yamamoto N, Kume T, Akaike A, Takahashi R, Shimohama S, Sawada H. Dopamine facilitates alpha-synuclein oligomerization in human neuroblastoma SH-SY5Y cells. Biochem Biophys Res Commun. 2010; 391:129–134. [PubMed: 19900407]
47. Wang W, Perovic I, Chittuluru J, Kaganovich A, Nguyen LT, Liao J, Auclair JR, Johnson D, Landeru A, Simorellis AK, Ju S, Cookson MR, Asturias FJ, Agar JN, Webb BN, Kang C, Ringe D, Petsko GA, Pochapsky TC, Hoang QQ. A soluble alpha-synuclein construct forms a dynamic tetramer. Proc Natl Acad Sci U S A. 2011; 108:17797–17802. [PubMed: 22006323]
48. Seo JH, Rah JC, Choi SH, Shin JK, Min K, Kim HS, Park CH, Kim S, Kim EM, Lee SH, Lee S, Suh SW, Suh YH. Alpha-synuclein regulates neuronal survival via Bcl-2 family expression and PI3/Akt kinase pathway. FASEB J. 2002; 16:1826–1828. [PubMed: 12223445]
49. Iwai A, Masliah E, Yoshimoto M, Ge N, Flanagan L, de Silva HA, Kittel A, Saitoh T. The precursor protein of non-A beta component of Alzheimer's disease amyloid is a presynaptic protein of the central nervous system. Neuron. 1995; 14:467–475. [PubMed: 7857654]
50. Borghi R, Marchese R, Negro A, Marinelli L, Forloni G, Zaccheo D, Abbruzzese G, Tabaton M. Full length alpha-synuclein is present in cerebrospinal fluid from Parkinson's disease and normal subjects. Neurosci Lett. 2000; 287:65–67. [PubMed: 10841992]
51. Burre J, Sharma M, Tsetsenis T, Buchman V, Etherton MR, Sudhof TC. Alpha-synuclein promotes SNARE-complex assembly in vivo and in vitro. Science. 2010; 329:1663–1667. [PubMed: 20798282]

52. Lashuel HA, Petre BM, Wall J, Simon M, Nowak RJ, Walz T, Lansbury PT Jr. Alpha-synuclein, especially the Parkinson's disease-associated mutants, forms pore-like annular and tubular protofibrils. J Mol Biol. 2002; 322:1089–1102. [PubMed: 12367530]
53. Zijlstra N, Blum C, Segers-Nolten IM, Claessens MM, Subramaniam V. Molecular composition of sub-stoichiometrically labeled alpha-synuclein oligomers determined by single-molecule photobleaching. Angew Chem Int Ed Engl. 2012; 51:8821–8824. [PubMed: 22806998]
54. Giehm L, Svergun DI, Otzen DE, Vestergaard B. Low-resolution structure of a vesicle disrupting α-synuclein oligomer that accumulates during fibrillation. Proc Natl Acad Sci U S A. 2011; 108:3246–3251. [PubMed: 21300904]
55. Winner B, Jappelli R, Maji SK, Desplats PA, Boyer L, Aigner S, Hetzer C, Loher T, Vilar M, Campioni S, Tzitzilonis C, Soragni A, Jessberger S, Mira H, Consiglio A, Pham E, Masliah E, Gage FH, Riek R. In vivo demonstration that alpha-synuclein oligomers are toxic. Proc Natl Acad Sci U S A. 2011; 108:4194–4199. [PubMed: 21325059]
56. Desplats P, Lee HJ, Bae EJ, Patrick C, Rockenstein E, Crews L, Spencer B, Masliah E, Lee SJ. Inclusion formation and neuronal cell death through neuron-to-neuron transmission of alpha-synuclein. Proc Natl Acad Sci U S A. 2009; 106:13010–13015. [PubMed: 19651612]
57. Shvadchak VV, Yushchenko DA, Pievo R, Jovin TM. The mode of alpha-synuclein binding to membranes depends on lipid composition and lipid to protein ratio. FEBS Lett. 2011; 585:3513–3519. [PubMed: 22004764]
58. Tosatto L, Andrighetti AO, Plotegher N, Antonini V, Tessari I, Ricci L, Bubacco L, Dalla Serra M. Alpha-synuclein pore forming activity upon membrane association. Biochim Biophys Acta. 2012; 1818:2876–2883. [PubMed: 22820150]
59. Feng LR, Federoff HJ, Vicini S, Maguire-Zeiss KA. Alpha-synuclein mediates alterations in membrane conductance: a potential role for alpha-synuclein oligomers in cell vulnerability. Eur J Neurosci. 2010; 32:10–17. [PubMed: 20550572]
60. Scott D, Roy S. alpha-Synuclein inhibits intersynaptic vesicle mobility and maintains recycling-pool homeostasis. J Neurosci. 2012; 32:10129–10135. [PubMed: 22836248]
61. Shavali S, Brown-Borg HM, Ebadi M, Porter J. Mitochondrial localization of alpha-synuclein protein in alpha-synuclein overexpressing cells. Neurosci Lett. 2008; 439:125–128. [PubMed: 18514418]
62. Gui YX, Wang XY, Kang WY, Zhang YJ, Zhang Y, Zhou Y, Quinn TJ, Liu J, Chen SD. Extracellular signal-regulated kinase is involved in alpha-synuclein-induced mitochondrial dynamic disorders by regulating dynamin-like protein 1. Neurobiol Aging. 2012; 33:2841–2854. [PubMed: 22445325]
63. Devi L, Raghavendran V, Prabhu BM, Avadhani NG, Anandatheerthavarada HK. Mitochondrial import and accumulation of alpha-synuclein impair complex I in human dopaminergic neuronal cultures and Parkinson disease brain. J Biol Chem. 2008; 283:9089–9100. [PubMed: 18245082]
64. Butler EK, Voigt A, Lutz AK, Toegel JP, Gerhardt E, Karsten P, Falkenburger B, Reinartz A, Winklhofer KF, Schulz JB. The mitochondrial chaperone protein TRAP1 mitigates alpha-Synuclein toxicity. PLoS Genet. 2012; 8:e1002488. [PubMed: 22319455]

Highlights

- αSyn is present in cell as a monomer and not as homotetramer
- αSyn oligomerizes in cells when it exceeds the threshold concentration of 90 nM
- Large αsyn aggregates are not present
- Oligomers are partially sequestered into lysosomes
- Mitochondria morphology is affected in the presence of αsyn oligomers

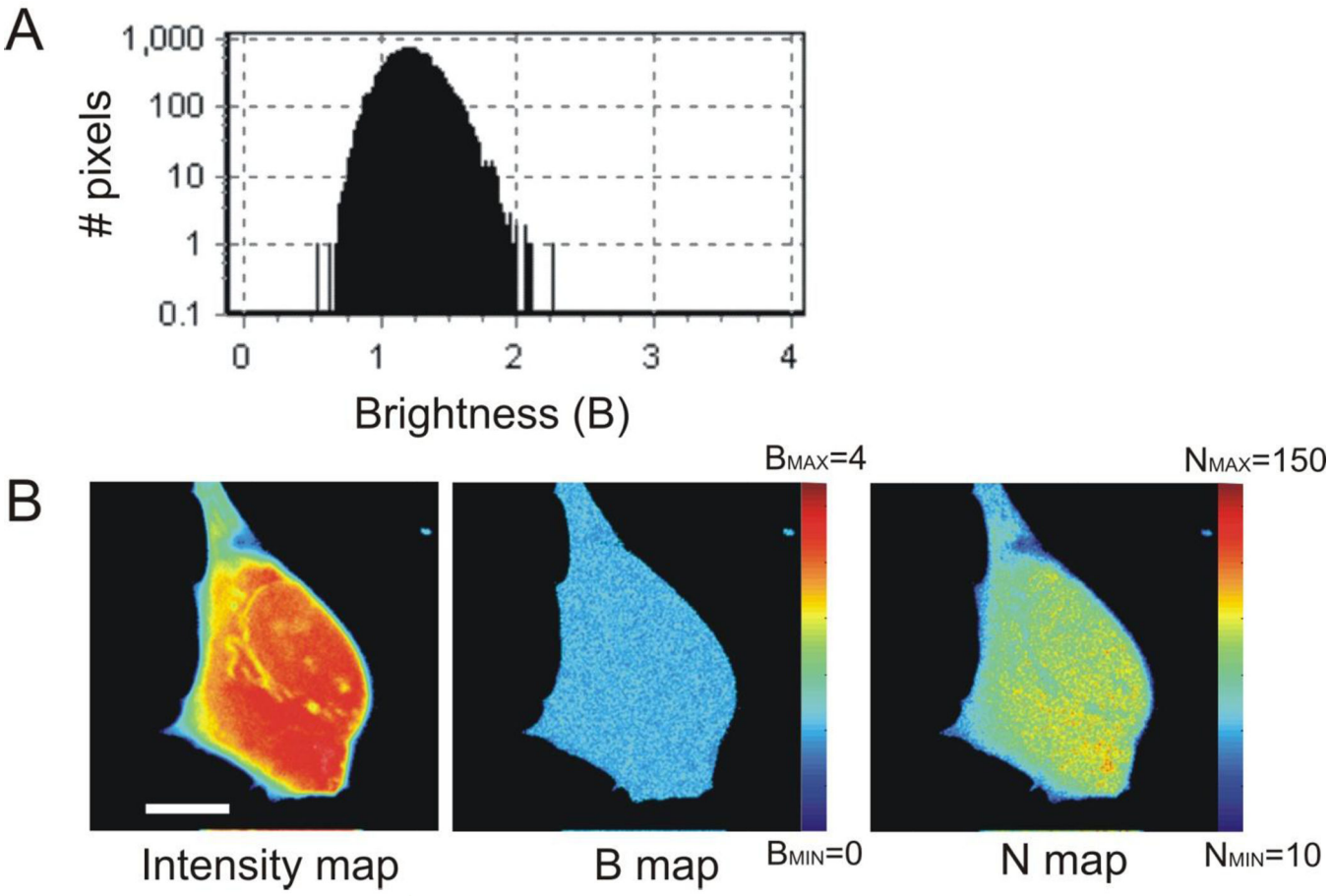

Figure 1. Determination of EGFP molecular brightness B

A. Distribution of the brightness B values of EGFP overexpressed in SH-SY5Y cells is centered at B=1.18±0.16 and identifies the brightness of EGFP monomer under these imaging conditions.

B. Average intensity image of a cell overexpressing EGFP (Intensity map), B map and N map representing respectively the average brightness B and the average apparent number of molecules N per pixel. The maps show a homogeneous B distribution in the cell cytoplasm, as expected, while the N value distribution in the cell varies in good agreement with the Intensity map (color scale, a. u). White bar 10 μm.

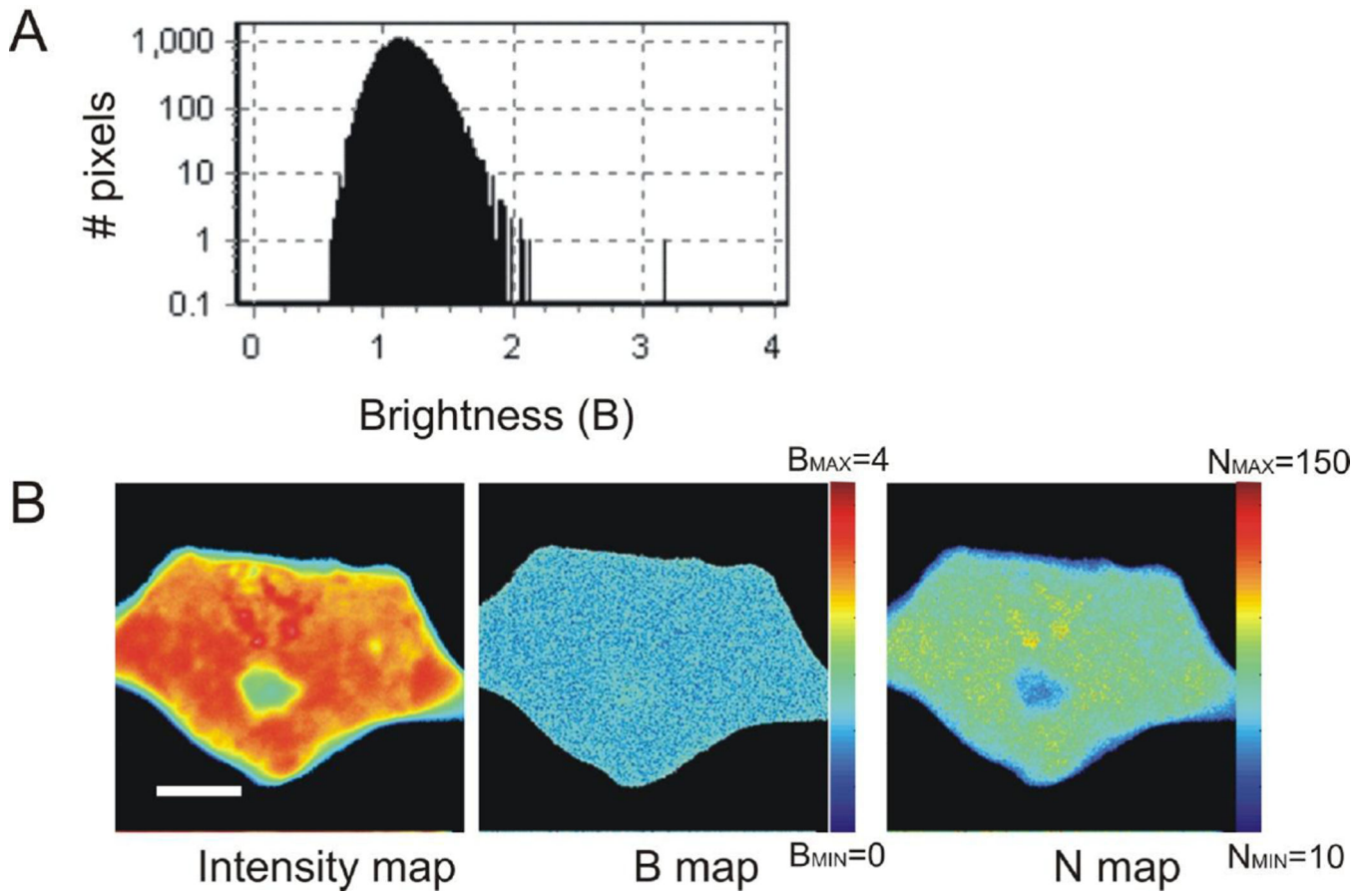

Figure 2. syn-EGFP is present as a monomer in overexpressing SH-SY5Y cells

A. Distribution of the brightness B of αsyn-EGFP overexpressed in SH-SY5Y cells is centered, as expected, at B=1.18 and identifies the brightness B of αsyn-EGFP in its monomeric form under these imaging conditions.

B. Average intensity image of a cell overexpressing αsyn-EGFP (Intensity map), B map and N map representing respectively the average brightness B and the average apparent number of molecules N per pixel. The maps show a homogeneous B distribution in the cell cytoplasm, meaning that αsyn-EGFP is monomeric in these conditions, while the N value distribution in the cell varies in good agreement with the Intensity map (color scale, a. u.). White bar 5 μm.

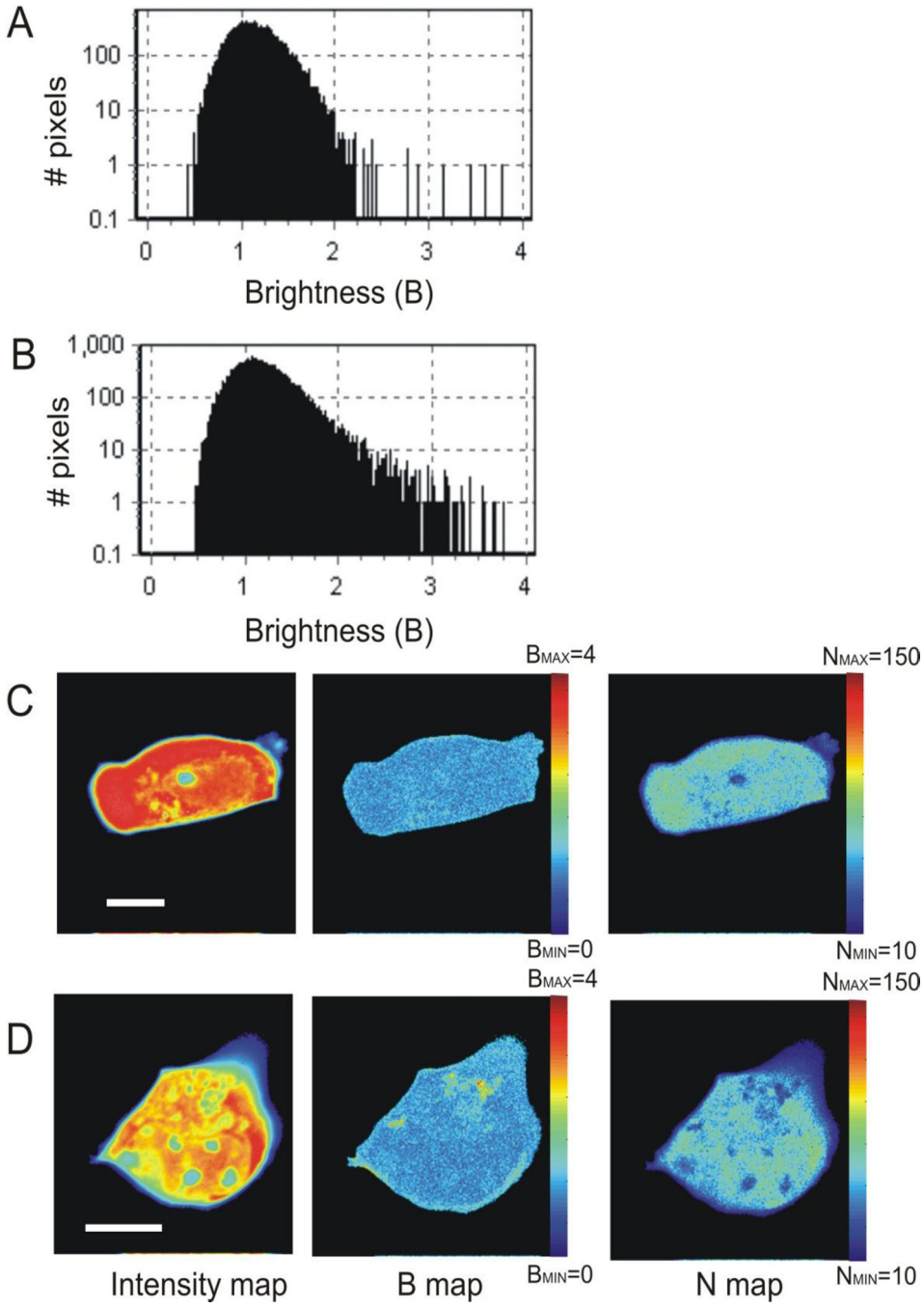

Figure 3. αsyn-EGFP can oligomerize in overexpressing SH-SY5Y cells

A. Distribution of the brightness B values of αsyn-EGFP overexpressed in SH-SY5Y cells starts to broaden at higher B values. This broadening represents pixels showing B values higher than 1.18 and therefore oligomeric species of αsyn-EGFP.

B. Distribution of the brightness B values of αsyn-EGFP overexpressed in SH-SY5Y cells shows a large broadening due to the presence of a larger amount of αsyn-EGFP oligomers. The B value distributions for the different oligomeric species cannot be separated from the B distribution for monomeric αsyn-EGFP, however calculating a weighted average of the B

values accounting for the oligomeric species we obtained about 1.95. This overall B value for the oligomers means that they are on average constituted by 6 αsyn-EGFP monomers. C. Average intensity image (Intensity map), B map and N map representing respectively the average brightness B and the average apparent number of molecules N per pixel of a cell overexpressing αsyn-EGFP, corresponding to the Brightness distribution represented in panel B. The maps show a homogeneous B value distribution in the cell cytoplasm, not really accounting for the slight broadening in the B histogram representing the oligomeric species. The N value distribution in the cell varies in the different regions in good agreement with the Intensity map(color scale, a. u.). White bar 10 μm.

D. Average intensity image (Intensity map), B map and N map representing respectively the average brightness B and the average apparent number of molecules N per pixel of a cell overexpressing αsyn-EGFP, corresponding to the Brightness distribution represented in panel B. The maps show a heterogeneous B value distribution in the cell cytoplasm, meaning that αsyn-EGFP formed oligomers. The N value distribution in the cell varies in good agreement with the Intensity map and where the B value is increased, the N value is lower than the average (color scale, a. u.). White bar 10 μm.

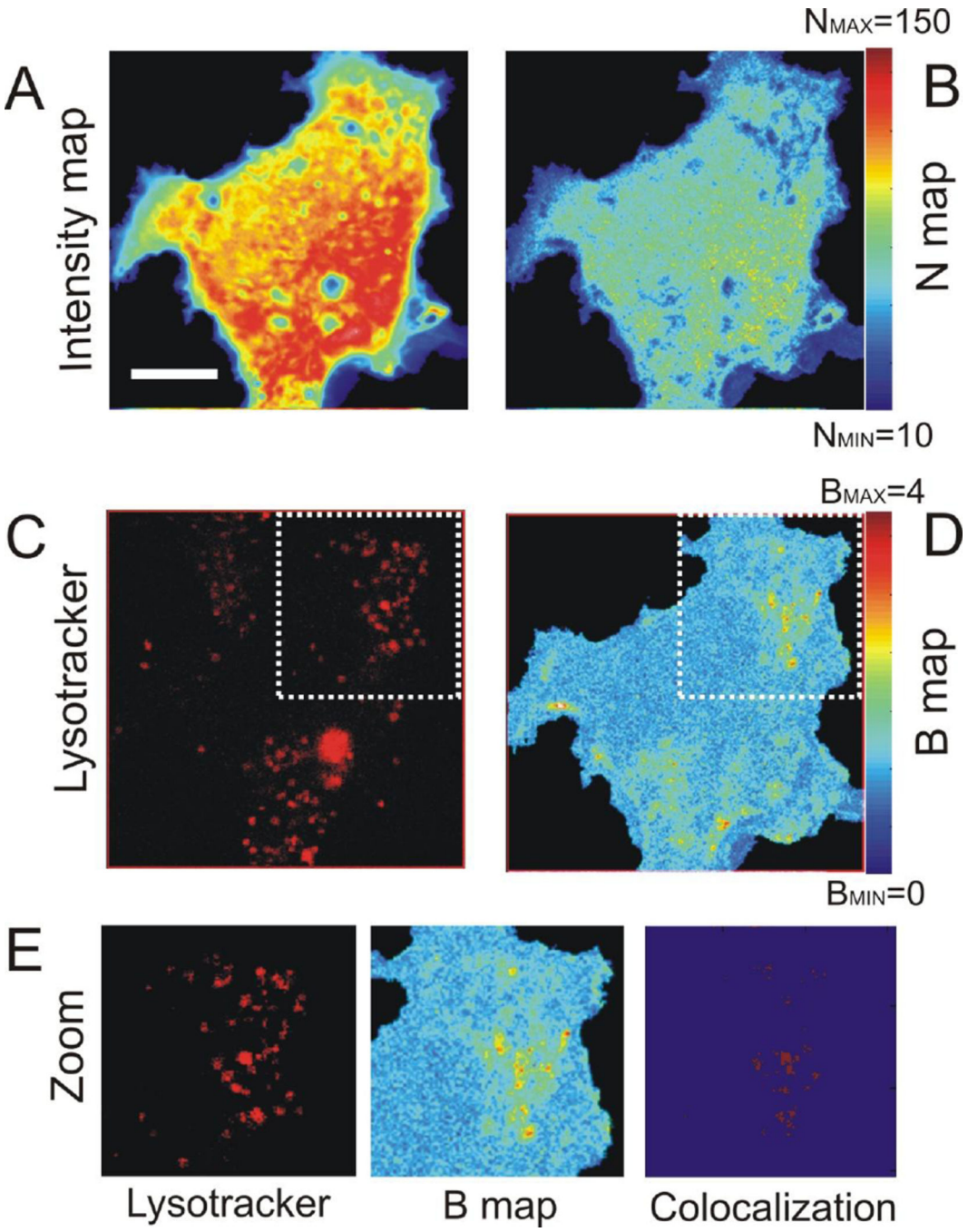

Figure 4. Lysotracker staining of a cell presenting αsyn-EGFP oligomers

Average intensity image (Intensity map), N map and B map of a cell overexpressing αsyn-EGFP (Panel A, B and D, respectively) and showing localized oligomeric species, in comparison with the same cell stained with Lysotracker (Panel C). In panel E a zoomed region for the Lysotracker image and for the B map is shown: on the right, pixels presenting colocalization between the pixels showing higher B values associated with the presence of oligomeric species and pixels positive to Lysotracker staining are represented in red on a

blue background and indicate that at least part of the αsyn-EGFP oligomers are sequestered into the lysosomes after ALP activation(color scale, a. u.). White bar 10 μm.

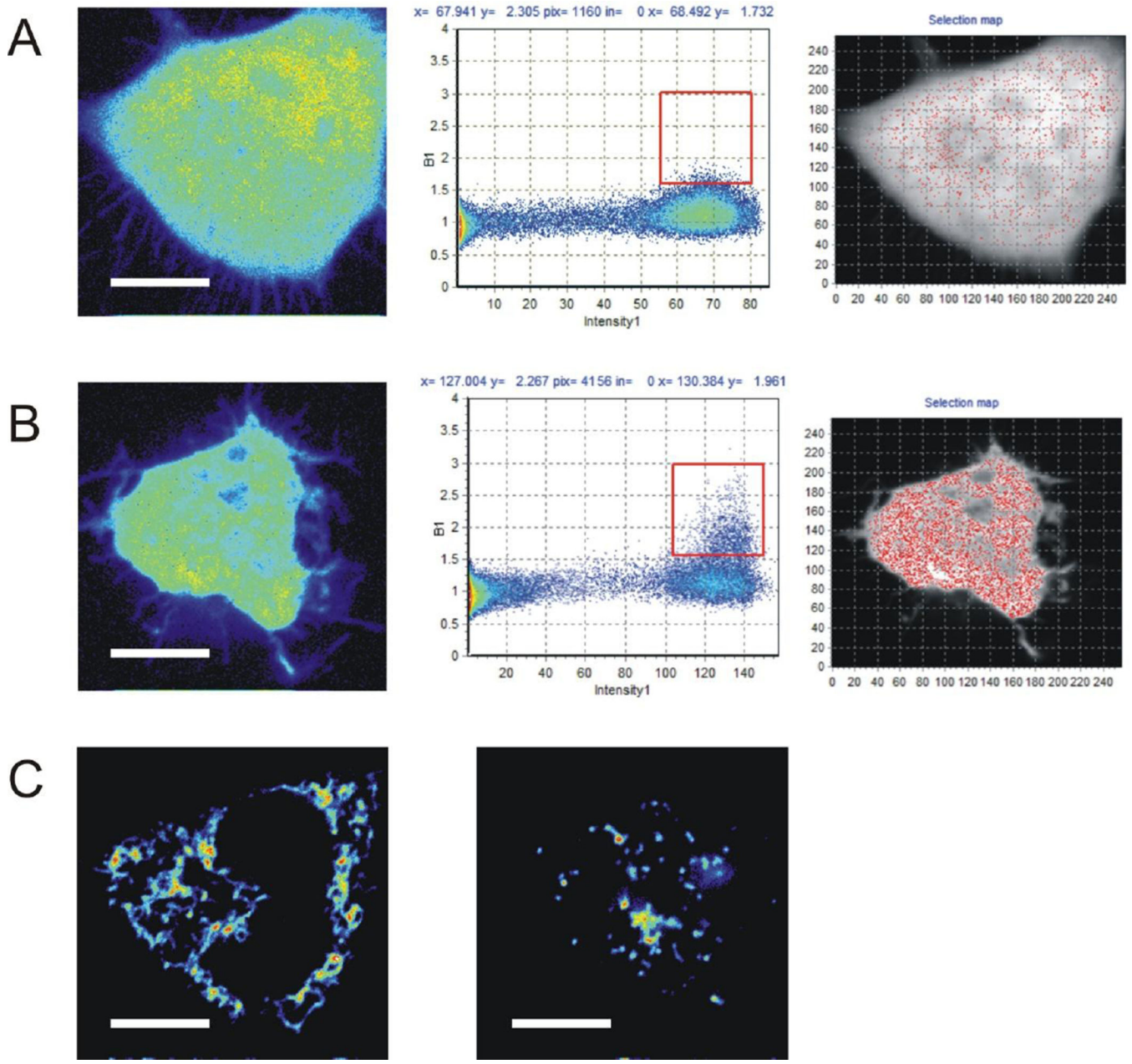

Figure 5. Mitochondrial staining highlights mitochondrial fragmentation in the presence of αsyn-EGFP oligomers

A. Intensity map of a cell overexpressing EGFP (left panel), as control (color scale, a. u.). Corresponding distribution of B values versus fluorescence intensity for the same cell (center panel), and associated Selection map where pixels selected with the red cursor in the B distribution are highlighted in red (right panel). The slightly higher B values in this case (red pixels in the right panel) are only accounting for the large FWHM of the B values distribution as shown in Figure 1A. White bar 10 μm.

B. Intensity map of a cell overexpressing αsyn-EGFP (left panel, color scale, a. u.). Corresponding distribution of B values versus fluorescence intensity for the same cell (center panel), and associated Selection map where pixels selected with the red cursor in the

B distribution are highlighted in red (right panel). The higher B values (red pixels in the right panel) represent the oligomeric species present in this cell. White bar 10 μm.
C. TMRE staining of the two cells showed in Figure 5A (left panel) and in Figure 5B (right panel). The mitochondrial morphology is clearly altered in the cell overexpressing αsyn-EGFP and showing αsyn-EGFP oligomers, compared to the overexpressing EGFP cell. White bar 10 μm.

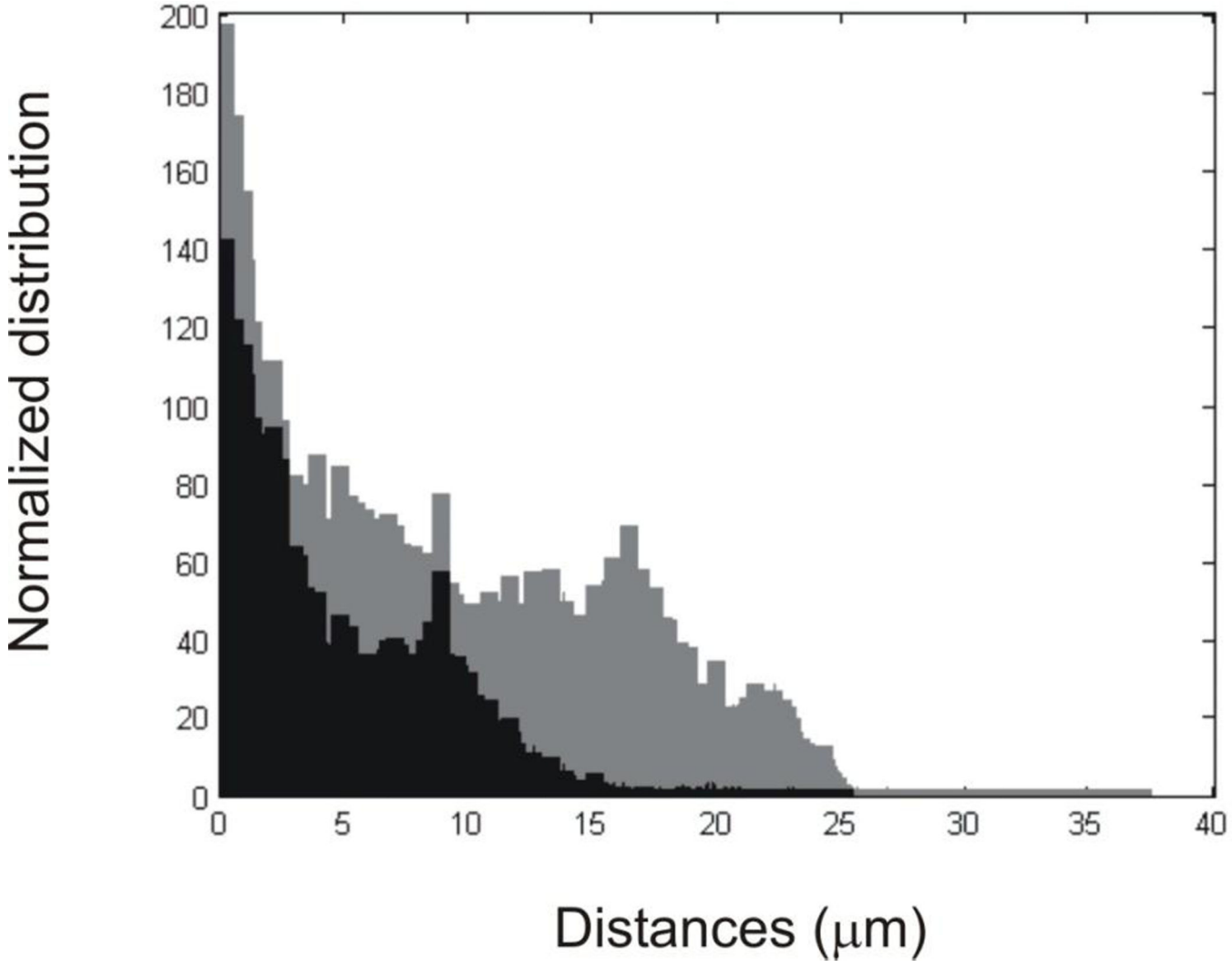

Figure 6. Distances distribution between pixels positive to mitochondria staining

The grey distribution represents the distances between pixels positive to mitochondrial staining in the cells overexpressing EGFP (correspondent to Figure 4C, left panel), while the black one shows the distances between pixels positive to mitochondrial staining in the cell overexpressing αsyn-EGFP and showing αsyn-EGFP oligomers (correspondent to Figure 4C, right panel). Both distributions are normalized by distribution area. The difference between the two distributions may account for mitochondrial fragmentation and alteration in mitochondria morphology and distribution in the cells cytoplasm.